

# Charge and transition form factors of light mesons in LFQM

C.-W. Hwang<sup>a</sup>

Department of Physics, National Tsing Hua University, Hsinchu 300, Taiwan

Received: 23 November 2000 / Revised version: 23 December 2000 /

Published online: 23 February 2001 – © Springer-Verlag 2001

**Abstract.** The charge and transition form factors of pions ( $F_\pi$ ,  $F_{\pi\gamma}$ , and  $F_{\pi\gamma^*}$ ) are studied in the light-front quark model (LFQM). We find that our results for  $F_\pi$  and  $F_{\pi\gamma}$  agree well with experiment. Furthermore, the mixing of  $\eta$  and  $\eta'$  is considered. We also calculate  $F_{\eta\gamma}$  and  $F_{\eta'\gamma}$  and compare them with the data.

## 1 Introduction

Form factors are important physical quantities in understanding the internal structure of hadrons. In this paper, we study two types of form factors: charge and transition form factors for some light mesons. The former is relevant in elastic electron meson scattering in which one off-shell photon exchanges between the electron and one of the quarks in the meson. The latter, on the other hand, comes from the reactions where the meson is produced by one on-shell and one off-shell photon. It is well known that these form factors must be treated with non-perturbative calculations. There are many different approaches to achieve this purpose, such as lattice calculations [1], vector meson dominance (VMD) [2,3], perturbative QCD (pQCD) with some non-perturbative inputs [4–7], QCD sum rules [8–10], nonlocal quark-pion dynamics [11], and the light-front quark model (LFQM) [12–20].

LFQM is the only relativistic quark model in which a consistent and fully relativistic treatment of quark spins and the center-of-mass motion can be carried out. Thus it has been applied in the past to calculate various form factors [12–20]. This model has many advantages. For example, the light-front wavefunction is manifestly boost invariant as it is expressed in terms of the momentum fraction variables (in the “+” component) in analogy to the parton distributions in the infinite momentum frame. Moreover, hadron spin can also be relativistically constructed by using the so-called Melosh rotation. The kinematic subgroup of the light-front formalism has the maximum number of interaction-free generators including the boost operator which describes the center-of-mass motion of the bound state (for a review of the light-front dynamics and light-front QCD, see [23]). For charge and transition form factors, we concentrate on the space-like region  $q^2 \leq 0$  ( $q$  being the momentum transfer). In this region, the so-called Z graph vanishes because we choose  $q^+ = 0$  [20–22], and only the valence quark contributes. We have a consistent treatment of the decay constants and of the charge and

transition form factors in LFQM. On the other hand, there are some experimental data which concern the charge [24–27] and transition [28] form factors for some light mesons. They will offer some tests of this approach.

This paper is organized as follows. In Sect. 2, the basic theoretical formalism is given and the decay constant and the charge and transition form factors are derived for pseudoscalar mesons. In Sect. 3, some asymptotic behaviors and the numerical results for some light mesons are presented and discussed. Finally, the conclusion is given in Sect. 4.

## 2 Framework

We will describe in this section the light-front approach for the calculation of the charge and transition form factors for off-shell photons and light mesons. The hadronic matrix elements are evaluated at space-like momentum transfer, namely the region  $q^2 \leq 0$ .

A meson bound state consisting of a quark  $q_1$  and an antiquark  $\bar{q}_2$  with total momentum  $P$  and spin  $S$  can be written as

$$\begin{aligned}
 & |M(P, S, S_z)\rangle \\
 &= \int \{d^3p_1\} \{d^3p_2\} 2(2\pi)^3 \delta^3(\tilde{P} - \tilde{p}_1 - \tilde{p}_2) \\
 &\quad \times \sum_{\lambda_1, \lambda_2} \Psi^{SS_z}(\tilde{p}_1, \tilde{p}_2, \lambda_1, \lambda_2) |q_1(p_1, \lambda_1) \bar{q}_2(p_2, \lambda_2)\rangle, \quad (1)
 \end{aligned}$$

where  $p_1$  and  $p_2$  are the on-mass-shell light-front momenta,

$$\tilde{p} = (p^+, p_\perp), \quad p_\perp = (p^1, p^2), \quad p^- = \frac{m^2 + p_\perp^2}{p^+}, \quad (2)$$

and

$$\{d^3p\} \equiv \frac{dp^+ d^2p_\perp}{2(2\pi)^3},$$

$$|q(p_1, \lambda_1) \bar{q}(p_2, \lambda_2)\rangle = b_{\lambda_1}^\dagger(p_1) d_{\lambda_2}^\dagger(p_2) |0\rangle, \quad (3)$$

<sup>a</sup> e-mail: v00570@phys.nthu.edu.tw

$$\begin{aligned} \{b_{\lambda'}(p'), b_{\lambda}^{\dagger}(p)\} &= \{d_{\lambda'}(p'), d_{\lambda}^{\dagger}(p)\} \\ &= 2(2\pi)^3 \delta^3(\vec{p}' - \vec{p}) \delta_{\lambda'\lambda}. \end{aligned}$$

In terms of the light-front relative momentum variables  $(x, k_{\perp})$  defined by

$$\begin{aligned} p_1^+ &= (1-x)P^+, & p_2^+ &= xP^+, \\ p_{1\perp} &= (1-x)P_{\perp} + k_{\perp}, & p_{2\perp} &= xP_{\perp} - k_{\perp}, \end{aligned} \quad (4)$$

the momentum-space wavefunction  $\Psi^{SS_z}$  can be expressed as

$$\Psi^{SS_z}(\vec{p}_1, \vec{p}_2, \lambda_1, \lambda_2) = R_{\lambda_1 \lambda_2}^{SS_z}(x, k_{\perp}) \phi(x, k_{\perp}), \quad (5)$$

where  $\phi(x, k_{\perp})$  describes the momentum distribution of the constituents in the bound state, and  $R_{\lambda_1 \lambda_2}^{SS_z}$  constructs a state of definite spin  $(S, S_z)$  out of light-front helicity  $(\lambda_1, \lambda_2)$  eigenstates. Explicitly,

$$\begin{aligned} R_{\lambda_1 \lambda_2}^{SS_z}(x, k_{\perp}) &= \sum_{s_1, s_2} \langle \lambda_1 | \mathcal{R}_M^{\dagger}(1-x, k_{\perp}, m_1) | s_1 \rangle \\ &\quad \times \langle \lambda_2 | \mathcal{R}_M^{\dagger}(x, -k_{\perp}, m_2) | s_2 \rangle \\ &\quad \times \left\langle \frac{1}{2} s_1; \frac{1}{2} s_2 | S, S_z \right\rangle, \end{aligned} \quad (6)$$

where  $|s_i\rangle$  are the usual Pauli spinors, and  $\mathcal{R}_M$  is the Melosh transformation operator:

$$\mathcal{R}_M(x, k_{\perp}, m_i) = \frac{m_i + xM_0 + i\sigma \cdot \mathbf{k}_{\perp} \times \mathbf{n}}{\sqrt{(m_i + xM_0)^2 + k_{\perp}^2}}, \quad (7)$$

with  $\mathbf{n} = (0, 0, 1)$ , a unit vector in the  $z$ -direction, and

$$M_0^2 = \frac{m_1^2 + k_{\perp}^2}{(1-x)} + \frac{m_2^2 + k_{\perp}^2}{x}. \quad (8)$$

In practice it is more convenient to use the covariant form for  $R_{\lambda_1 \lambda_2}^{SS_z}$  [14]:

$$R_{\lambda_1 \lambda_2}^{SS_z}(x, k_{\perp}) = \frac{\sqrt{p_1^+ p_2^+}}{\sqrt{2\widetilde{M}_0}} \bar{u}(p_1, \lambda_1) \Gamma v(p_2, \lambda_2), \quad (9)$$

where

$$\begin{aligned} \widetilde{M}_0 &\equiv \sqrt{M_0^2 - (m_1 - m_2)^2}, \\ \Gamma &= \gamma_5 \quad (\text{pseudoscalar}, S=0). \end{aligned} \quad (10)$$

We normalize the meson state as

$$\begin{aligned} \langle M(P', S', S'_z) | M(P, S, S_z) \rangle \\ = 2(2\pi)^3 P^+ \delta^3(\vec{P}' - \vec{P}) \delta_{S'S} \delta_{S'_z S_z}, \end{aligned} \quad (11)$$

so that

$$\int \frac{dx d^2 k_{\perp}}{2(2\pi)^3} |\phi(x, k_{\perp})|^2 = 1. \quad (12)$$

In principle, the momentum distribution amplitude  $\phi(x, k_{\perp})$  can be obtained by solving the light-front QCD bound state equation [23, 29]. However, before such first-principles solutions are available, we shall have to be contented with phenomenological amplitudes. One example that has often been used in the literature for heavy mesons is the Gaussian-type wavefunction,

$$\phi(x, k_{\perp})_G = \mathcal{N} \sqrt{\frac{dk_z}{dx}} \exp\left(-\frac{\mathbf{k}^2}{2\omega^2}\right), \quad (13)$$

where  $\mathcal{N} = 4(\pi/\omega^2)^{3/4}$  and  $k_z$  is the internal momentum  $\mathbf{k} = (\mathbf{k}_{\perp}, k_z)$ , defined through

$$1-x = \frac{e_1 - k_z}{e_1 + e_2}, \quad x = \frac{e_2 + k_z}{e_1 + e_2}, \quad (14)$$

with  $e_i = (m_i^2 + \mathbf{k}^2)^{1/2}$ . We then have

$$M_0 = e_1 + e_2, \quad k_z = \frac{xM_0}{2} - \frac{m_2^2 + k_{\perp}^2}{2xM_0}, \quad (15)$$

and

$$\frac{dk_z}{dx} = \frac{e_1 e_2}{x(1-x)M_0}, \quad (16)$$

which is the Jacobian of the transformation from  $(x, k_{\perp})$  to  $\mathbf{k}$ . This wavefunction has been also used in many other studies of hadronic transitions. Besides this wavefunction which has the exponential form, we also consider one of power-law type:

$$\phi(x, k_{\perp})_N = \mathcal{N} \left( \frac{\omega^2}{M_0^2 + \omega^2} \right)^n. \quad (17)$$

where  $n$  is another parameter. In this paper, we only consider the light mesons: the  $u$  and  $d$  quark masses are the same ( $m_u = m_d = m_q$ ), thus (8) will be reduced to

$$M_0^2 = \frac{m_q^2 + k_{\perp}^2}{x(1-x)}. \quad (18)$$

Thus, the  $k_{\perp}$ -dependence of the wavefunction  $\phi(x, k_{\perp})_N$  occurs exclusively in the combination  $k_{\perp}^2/x(1-x)$ , which is consistent with the conditions in [30, 31]. We will calculate the results by using these two wavefunctions and compare them with the data.

## 2.1 Decay constants

The decay constants of pseudoscalar mesons  $P(q_1 \bar{q}_2)$  which include octet and singlet are defined by

$$\begin{aligned} \langle 0 | A_{\mu}^a | P(p) \rangle &= \sqrt{2} i f_P^a p_{\mu} \\ (a &= 1, \dots, 8, 0; P = \pi, K, \eta, \eta'), \end{aligned} \quad (19)$$

where  $A_{\mu}^a$  is the axial vector current. It can be evaluated using the light-front wavefunction given by (2.1) and (2.5)

$$\begin{aligned} \langle 0 | \bar{q}_2 \gamma^+ \gamma_5 q_1 | P \rangle &= \int \{d^3 p_1\} \{d^3 p_2\} 2(2\pi)^3 \\ &\quad \times \delta^3(\vec{p} - \vec{p}_1 - \vec{p}_2) \phi_P(x, k_{\perp}) R_{\lambda_1 \lambda_2}^{00}(x, k_{\perp}) \\ &\quad \times \langle 0 | \bar{q}_2 \gamma^+ \gamma_5 q_1 | q_1 \bar{q}_2 \rangle. \end{aligned} \quad (20)$$

Since  $\widetilde{M}_0(x(1-x))^{1/2} = (\mathcal{A}^2 + k_{\perp}^2)^{1/2}$ , it is straightforward to show that

$$f_P^a = 2\sqrt{3} \int \frac{dx d^2 k_{\perp}}{2(2\pi)^3} \phi_P(x, k_{\perp}) \frac{\mathcal{A}}{\sqrt{\mathcal{A}^2 + k_{\perp}^2}}, \quad (21)$$

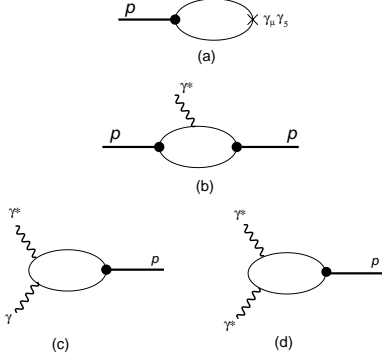


**Fig. 1a–d.** Diagrams for **a** one pseudoscalar meson decay to vacuum, **b** the scattering of one virtual photon and one meson, **c** a meson produced by one on-shell and one off-shell photons, and **d** a meson produced by two off-shell photons

where

$$\mathcal{A} = m_1 x + m_2(1 - x). \quad (22)$$

Note that the factor  $3^{1/2}$  in (21) arises from the color factor implicit in the meson wavefunction. We illustrate this process in Fig. 1a. Once the decay constant is known, it can be used to constrain the parameters appearing in the light-front wavefunction.

## 2.2 Charge form factors

The charge form factor of a pseudoscalar meson  $P$  is determined by the scattering of one virtual photon and one meson. This process is illustrated in Fig. 1b. This form factor can be defined by the matrix element

$$\langle P(p') | J^\mu | P(p) \rangle = F_P(Q^2)(p + p')^\mu, \quad (23)$$

where  $J^\mu$  is the vector current and  $Q^2 \equiv -q^2 = -(p - p')^2$ . As discussed in the above subsection, we readily obtain

$$\begin{aligned} \langle P(p') | \bar{q} \gamma^\mu q | P(p) \rangle = & \sum_{\lambda_1, \lambda'_1, \lambda_2, \lambda'_2} \int \{d^3 p_1\} \{d^3 p_2\} 2(2\pi)^3 \delta^3(\tilde{p} - \tilde{p}_1 - \tilde{p}_2) \\ & \times \phi_P^*(x, k'_\perp) \phi_P(x, k_\perp) R_{\lambda'_1 \lambda'_2}^{00\dagger} R_{\lambda_1 \lambda_2}^{00}, \end{aligned} \quad (24)$$

where  $k'_\perp \equiv k_\perp + xq_\perp$ . Comparing (23) with (24), we obtain

$$\begin{aligned} F_P(Q^2) = & \int \frac{dx d^2 k_\perp}{2(2\pi)^3} \phi_P^*(x, k'_\perp) \phi_P(x, k_\perp) \\ & \times \frac{\widetilde{M}_0}{\widetilde{M}'_0} \left( 1 + \frac{xq_\perp \cdot k_\perp}{\mathcal{A}^2 + k_\perp^2} \right), \end{aligned} \quad (25)$$

where  $\widetilde{M}'_0 \equiv (M_0'^2 - (m_1 - m_2)^2)^{1/2}$  and

$$M_0'^2 = \frac{m_1^2 + k_\perp'^2}{(1-x)} + \frac{m_2^2 + k_\perp^2}{x}. \quad (26)$$

This result is the same as (17) in [12]. Thus, the charge form factor  $F_P(Q^2)$  will become available once the parameters in the wavefunction are determined.

## 2.3 Transition form factors

There are two types of transition form factors:  $F_{\pi\gamma}$  and  $F_{\pi\gamma^*}$ . The form factor  $F_{P\gamma}$ , in which the meson is produced by one on-shell and one off-shell photon ( $\gamma\gamma^* \rightarrow P$ ), is defined by the  $P\gamma\gamma^*$  vertex [4]

$$\Gamma_\mu = -ie^2 F_{P\gamma}(Q^2) \varepsilon_{\mu\nu\rho\sigma} p^\nu q^\rho \epsilon^\sigma, \quad (27)$$

where  $q$  is the momentum of the off-shell photon,  $q^2 = -q_\perp^2 = -Q^2$ , and  $\epsilon$  is the polarization vector of the on-shell photon. We illustrate this process in Fig. 1c and write down the amplitude within the light-front framework [4]

$$\begin{aligned} \Gamma_\mu = & \sum_{\lambda_1, \lambda_2, \lambda} e_q e_{\bar{q}'} e^2 \int \{d^3 p_1\} \{d^3 p_2\} \\ & \times 2(2\pi)^3 \delta^3(\tilde{p} - \tilde{p}_1 - \tilde{p}_2) \phi_P(x, k_\perp) \\ & \times \left[ \left( \frac{q_\perp^2}{p^+} - \frac{m_1^2 + (k_\perp + q_\perp)^2}{p_1^+} - \frac{m_2^2 + k_\perp^2}{p_2^+} \right)^{-1} \right. \\ & \times \bar{v}(p_2, \lambda_2) \not{\epsilon} u(p'_1, \lambda) \bar{u}(p'_1, \lambda) \gamma_\mu u(p_1, \lambda_1) \\ & \left. + (1 \leftrightarrow 2) \right] R_{\lambda_1 \lambda_2}^{00}, \end{aligned} \quad (28)$$

where  $e_q$  and  $e_{\bar{q}'}$  are the electric charges of the quark  $q$  and  $\bar{q}'$ , respectively. It is straightforward to show that

$$\begin{aligned} F_{P\gamma}(Q^2) = & -4 \frac{\sqrt{3}}{\sqrt{2}} e_q e_{\bar{q}'} \int \frac{dx d^2 k_\perp}{2(2\pi)^3} \phi_P(x, k_\perp) \frac{\mathcal{A}}{\sqrt{\mathcal{A}^2 + k_\perp^2}} \\ & \times \left[ \frac{1}{(1-x) \left( q_\perp^2 - \frac{m_1^2 + (k_\perp + q_\perp)^2}{1-x} - \frac{m_2^2 + k_\perp^2}{x} \right)} \right. \\ & \left. + \frac{1}{x \left( q_\perp^2 - \frac{m_1^2 + k_\perp^2}{1-x} - \frac{m_2^2 + (k_\perp - q_\perp)^2}{x} \right)} \right]. \end{aligned} \quad (29)$$

This result is consistent with (4.4) of [32]. The form factor  $F_{P\gamma^*}$  arising from the  $P\gamma^*\gamma^*$  vertex, where  $\gamma^*\gamma^*$  represents two off-shell photons, is defined by [33]

$$\Gamma_{\mu\nu} = -ie^2 F_{P\gamma^*}(Q^2, Q'^2) \varepsilon_{\mu\nu\rho\sigma} \mathcal{Q}^\rho \mathcal{P}^\sigma, \quad (30)$$

where  $\mathcal{Q} \equiv (1/2)(q' - q)$ ,  $\mathcal{P} \equiv q' + q$ , and  $Q'^2 = -q'^2 = q_\perp'^2$ . This process is depicted in Fig. 1d. We expect that this amplitude is similar to the one off-shell photon case and that it has the form

$$\begin{aligned} \Gamma_{\mu\nu} = & \sum_{\lambda_1, \lambda_2, \lambda} e_q e_{\bar{q}'} e^2 \int \{d^3 p_1\} \{d^3 p_2\} \\ & \times 2(2\pi)^3 \delta^3(\tilde{p} - \tilde{p}_1 - \tilde{p}_2) \phi_P(x, k_\perp) \\ & \times \left[ \left( \frac{q_\perp^2 - q_\perp'^2}{p^+} - \frac{m_1^2 + (k_\perp + q_\perp)^2}{p_1^+} - \frac{m_2^2 + k_\perp^2}{p_2^+} \right)^{-1} \right. \\ & \times \bar{v}(p_2, \lambda_2) \gamma_\nu u(p'_1, \lambda) \bar{u}(p'_1, \lambda) \gamma_\mu u(p_1, \lambda_1) \\ & \left. + (1 \leftrightarrow 2) \right] R_{\lambda_1 \lambda_2}^{00}. \end{aligned} \quad (31)$$

From (30) and (31), we arrive at

$$\begin{aligned}
& F_{P\gamma^*}(Q^2, Q'^2) \\
&= -4 \frac{\sqrt{3}}{\sqrt{2}} e_q e_{q'} \int \frac{dx d^2 k_\perp}{2(2\pi)^3} \phi_P(x, k_\perp) \frac{\mathcal{A}}{\sqrt{\mathcal{A}^2 + k_\perp^2}} \\
&\times \left[ \frac{1}{(1-x) \left( q_\perp^2 - q'_\perp^2 - \frac{m_1^2 + (k_\perp + q_\perp)^2}{1-x} - \frac{m_2^2 + k_\perp^2}{x} \right)} \right. \\
&\left. + \frac{1}{x \left( q_\perp^2 - q'_\perp^2 - \frac{m_1^2 + k_\perp^2}{1-x} - \frac{m_2^2 + (k_\perp - q_\perp)^2}{x} \right)} \right]. \quad (32)
\end{aligned}$$

### 3 Numerical results and discussions

We now compare our results for the form factors with the experimental data. Before doing this, we need to determine the parameters  $m_1$ ,  $m_2$ , and  $\omega$  appearing in the wavefunction  $\phi_P(x, k_\perp)$ . Of course, we assume that this wavefunction is process-independent.

In the  $\pi\text{-}\gamma$  case, the constituent masses of the  $u$  and  $d$  quarks are the same, i.e.,  $m_u = m_d \equiv m_q$ . We can use the experimental value for the decay constant,  $f_\pi = 92.4 \text{ MeV}$  [35] to determine the parameters  $m_q$  and  $\omega_\pi$  via (21). However, there is more than one parameter to be determined from one experimental value. Therefore, in principle we have infinite combinations satisfying the decay constant value. If we can find other constraints, these parameters will be determined uniquely. The charge form factor of the pion has the following low-energy expansion:

$$F_\pi(Q^2) = 1 + \frac{1}{6} \langle r^2 \rangle_\pi Q^2 + O(Q^4), \quad (33)$$

where  $\langle r^2 \rangle_\pi$  is the electromagnetic radius of the charged pion. Thus,

$$\langle r^2 \rangle_\pi \simeq -6 \left. \frac{\partial F_\pi(Q^2)}{\partial Q^2} \right|_{Q^2=0}. \quad (34)$$

Experimentally one finds [34]

$$\langle r^2 \rangle_\pi^{\text{exp}} = (0.439 \pm 0.03) \text{ fm}^2. \quad (35)$$

This offers the second constraint. The third one is from the transition form factor  $F_{\pi\gamma}(Q^2)$  (29); if we consider the limit  $Q^2 \rightarrow 0$ , there is the simple form

$$\begin{aligned}
F_{\pi\gamma}(0) &= 4 \frac{\sqrt{3}}{\sqrt{2}} \frac{(e_u^2 - e_d^2)}{\sqrt{2}} \int \frac{dx d^2 k_\perp}{2(2\pi)^3} \phi_\pi(x, k_\perp) \frac{\mathcal{A}}{\sqrt{\mathcal{A}^2 + k_\perp^2}} \\
&\times \left[ \frac{1}{x(1-x)M_0^2} \right]. \quad (36)
\end{aligned}$$

It is well known that  $F_{\pi\gamma}(0)$  is related to the decay width  $\Gamma(\pi \rightarrow \gamma\gamma)$  by [28]

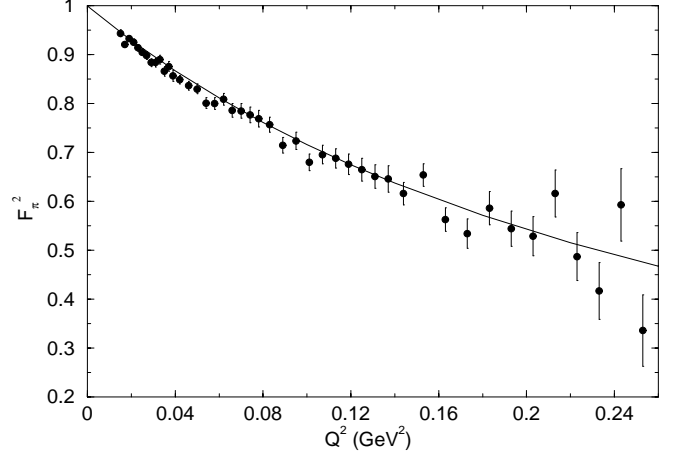


**Fig. 2.** The charge form factor of the pion in small momentum transfer. Data are taken from [24]

$$|F_{\pi\gamma}(0)|^2 = \frac{1}{(4\pi\alpha)^2} \frac{64\pi\Gamma(\pi \rightarrow \gamma\gamma)}{M_\pi^3}, \quad (37)$$

where  $\alpha$  is the QED coupling constant and  $M_\pi$  is the mass of the pion. From the experimental data for  $\Gamma(\pi \rightarrow \gamma\gamma)$  [35], one can obtain the value of  $F_{\pi\gamma}(0)$ :  $0.27 \pm 0.01 \text{ GeV}^{-1}$ . Besides (37),  $F_{\pi\gamma}(0)$  also can be determined from the axial anomaly in the chiral limit of QCD [36]:

$$F_{\pi\gamma}(Q^2)|_{Q^2 \rightarrow 0} = \frac{3\sqrt{2}C_\pi}{4\pi^2 f_\pi}. \quad (38)$$

where  $C_\pi = 1/(3(2^{1/2}))$ .

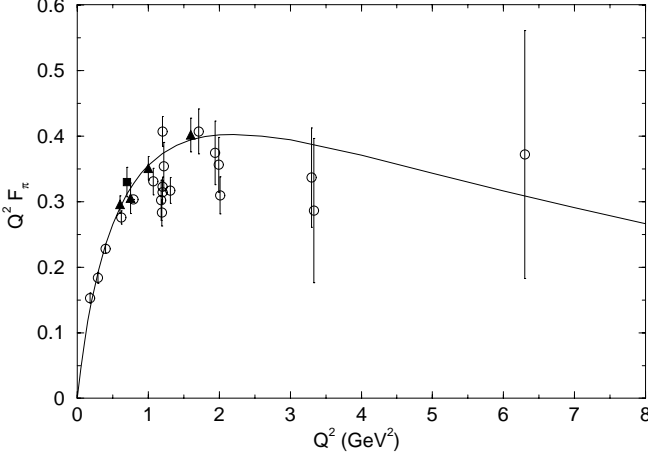
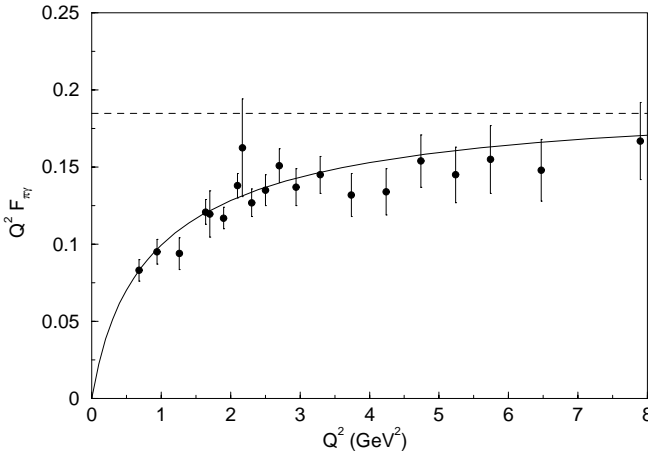
Thus, we can uniquely determine all the parameters in the wavefunction by using (21), (34), and (36). Here we list the fitted parameters of these two wavefunctions  $\phi_G$  and  $\phi_N$  in Table 1.

From Table 1, we find that the value  $F_{\pi\gamma}(0) = 0.27 \text{ GeV}^{-1}$  cannot be reached by adjusting the parameters  $m_q$  and  $\omega_\pi$  in the wavefunctions  $\phi_G$ . The reason may be that the transverse momentum suppression of the exponential forms in  $\phi_G$  are stronger than  $\phi_N$ . Thus we only use the type of wavefunction  $\phi(x, k_\perp)_N$  to calculate the form factors  $F_\pi(Q^2)$  and  $F_{\pi\gamma}(Q^2)$  in the  $-8 \text{ GeV}^2 \leq q^2 \leq 0$  region by using (25) and (29). On the one hand, the value of the parameter  $m_q = 0.192 \text{ GeV}$  is consistent with the order of the constituent quark mass,  $0.2 \sim 0.3 \text{ GeV}$ ; on the other hand, the fitted size of the charge pion,  $\langle r^2 \rangle_\pi = 0.434 \text{ fm}^2$ , almost equals the experimental value. Now, we have no degree of freedom to adjust this wavefunction because all the parameters have been fixed. From Figs. 2, 3, and 4, we find that these predictions are all in agreement with the experimental data [24, 25, 28].

There exist various models or methods that can be used to calculate these form factors. For  $F_\pi(Q^2)$ , [17] has used the Gaussian-type and power-law-type ( $n = 2$ ) wavefunction for small  $q^2$  region, [18] has used the Gaussian-type one for large  $q^2$  region; their results are fit the data well. The pion Bethe-Salpeter amplitude is completely analyzed in [37] and some nice results at small and large momentum transfers are obtained. The authors of [38] use the

**Table 1.** Parameters  $m_q$  and  $\omega_\pi$  in the  $\phi_G$  and  $\phi_N$  wavefunctions

| wavefunction    | $m_q$ (GeV) | $\omega_\pi$ (GeV) | $f_\pi$ (MeV) | $\langle r^2 \rangle_\pi$ (fm <sup>2</sup> ) | $F_{\pi\gamma}(0)$ (GeV <sup>-1</sup> ) |
|-----------------|-------------|--------------------|---------------|--|---|
| $\phi_G$        | 0.243       | 0.328              | 92.4          | 0.434  | 0.231                                   |
| $\phi_N(n=1.7)$ | 0.192       | 0.957              | 92.4          | 0.434  | 0.272                                   |

**Fig. 3.** The charge form factor of the pion in large momentum transfer. Data are taken from [25] (empty circles), [26] (filled triangles), and [27] (filled square)**Fig. 4.** The one off-shell photon transition form factor of the pion. The dotted line is the limiting behavior for  $2f_\pi$  (0.185 GeV) which is predicted by pQCD. Data are taken from [28]

pQCD approach to obtain the results in the  $Q^2 \geq 4 \text{ GeV}^2$  region.

For  $F_{\pi\gamma}(Q^2)$ , [18] has used the Gaussian-type wavefunction and the axial anomaly plus PCAC relations to calculate the decay width  $\Gamma(\pi \rightarrow \gamma\gamma)$ . The  $q^2$  dependence is derived in [32] and the numerical results are in agreement with the data. The method of pQCD also fits [39, 40] the data well in the  $-8 \text{ GeV}^2 \leq q^2 \leq -0.5 \text{ GeV}^2$  region. It is worth remarking here that pQCD predicts that the asymptotic behavior of  $F_{\pi\gamma}(Q^2)$  is proportional to the integration of  $[x(1-x)Q^2]^{-1}$  [4], that is,

$$Q^2 F_{\pi\gamma}(Q^2)|_{Q^2 \rightarrow \infty} \rightarrow \text{constant}; \quad (39)$$

it also has this property in (29).

For  $F_{\pi\gamma^*}(Q^2, Q'^2)$ , since there are no experimental data yet, we must proceed carefully. On the one hand, if the limit  $Q'^2 \rightarrow 0$  is taken, this form factor must be reduced to  $F_{\pi\gamma}(Q^2)$ . Indeed, this condition is satisfied in (32). On the other hand, if we take the limits  $Q^2, Q'^2 \rightarrow \infty$  and assume that the wavefunction  $\phi_\pi(x, k_\perp)$  is symmetric in  $x$  and  $1-x$ , the asymptotic behavior of the transition form factor (32) becomes

$$F_{\pi\gamma^*}(Q^2, Q'^2)|_{Q^2, Q'^2 \rightarrow \infty} = \frac{4}{\sqrt{3}} \int \frac{dx d^2 k_\perp}{2(2\pi)^3} \phi_\pi(x, k_\perp) \times \frac{\mathcal{A}}{\sqrt{\mathcal{A}^2 + k_\perp^2}} \left[ \frac{1}{xQ^2 + (1-x)Q'^2} \right], \quad (40)$$

which is also consistent with the assumption made in pQCD [6]. Thus we have confidence in the prediction of the values of  $F_{\pi\gamma^*}(Q^2, Q'^2)$  in terms of (32).

We also consider the  $\eta$ - $\eta'$  system. Due to the mixing in this system,  $\eta$  and  $\eta'$  both have  $\eta_8$  and  $\eta_0$  components. Recent investigations [41, 42] have shown that this system can adequately be described with two mixing angles,  $\theta_8$  and  $\theta_0$ . As has become clearer very recently [43, 44], a linear combination of orthogonal states  $\eta_q$  and  $\eta_s$  was made for the description of  $\eta$  and  $\eta'$ :

$$\begin{pmatrix} \eta \\ \eta' \end{pmatrix} = U(\alpha) \begin{pmatrix} \eta_q \\ \eta_s \end{pmatrix}, \quad U(\alpha) = \begin{pmatrix} \cos \alpha & -\sin \alpha \\ \sin \alpha & \cos \alpha \end{pmatrix}, \quad (41)$$

where  $\eta_q$  and  $\eta_s$  are composed of the valence quarks  $q\bar{q} = (u\bar{u} + d\bar{d})/2^{1/2}$  and  $s\bar{s}$ , respectively. The decay constants of  $\eta$  and  $\eta'$  are defined by

$$\langle 0 | A_\mu^j | P \rangle = \sqrt{2} i f_P^j p_\mu \quad (j = q, s; P = \eta, \eta'), \quad (42)$$

where  $A_\mu^q = (\bar{u}\gamma_\mu\gamma_5 u + \bar{d}\gamma_\mu\gamma_5 d)/2^{1/2}$  and  $A_\mu^s = \bar{s}\gamma_\mu\gamma_5 s$  both differ from (19) slightly. Thus,

$$\begin{pmatrix} f_\eta^q & f_\eta^s \\ f_{\eta'}^q & f_{\eta'}^s \end{pmatrix} = U(\alpha) \begin{pmatrix} f_q & 0 \\ 0 & f_s \end{pmatrix}. \quad (43)$$

Within this  $q\bar{q}$ - $s\bar{s}$  mixing scheme, the transition form factors  $F_{\eta\gamma}(Q^2)$  and  $F_{\eta'\gamma}(Q^2)$  in the limit  $Q^2 \rightarrow 0$  are analogous to (38) [44]

$$F_{\eta\gamma}(Q^2)|_{Q^2 \rightarrow 0} = \frac{3\sqrt{2}C_q}{4\pi^2 f_q} \cos \alpha - \frac{3\sqrt{2}C_s}{4\pi^2 f_s} \sin \alpha, \\ F_{\eta'\gamma}(Q^2)|_{Q^2 \rightarrow 0} = \frac{3\sqrt{2}C_q}{4\pi^2 f_q} \sin \alpha + \frac{3\sqrt{2}C_s}{4\pi^2 f_s} \cos \alpha, \quad (44)$$

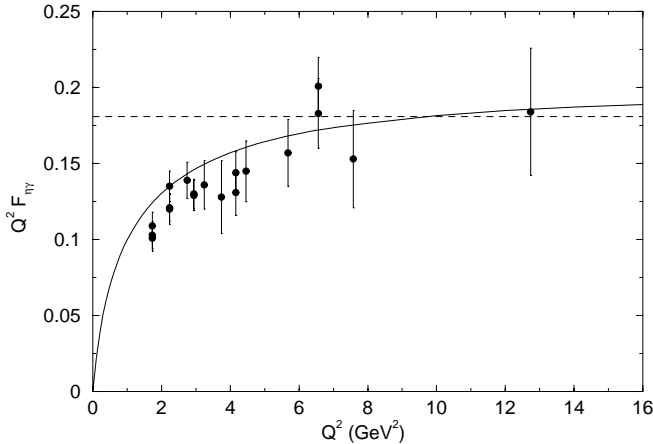


**Fig. 5.** The one off-shell photon transition form factor of  $\eta$ . The dotted line is the limiting behavior (0.182 GeV) which is predicted by pQCD. Data are taken from [28]

where  $C_q = 5/(9(2^{1/2}))$  and  $C_s = 1/9$ . For the wavefunctions  $\phi_{\eta_q}(x, k_\perp)$  and  $\phi_{\eta_s}(x, k_\perp)$ , there are four parameters  $m_q$ ,  $\omega_{\eta_q}$ ,  $m_s$ , and  $\omega_{\eta_s}$ . The value of  $m_q$  is fixed in the pion case, thus we need three constraints to determine the other three parameters uniquely. The authors of [43], after considering the data of the decay widths  $\Gamma(\eta^{(\prime)} \rightarrow \gamma\gamma)$  and some other processes, obtain

$$\begin{aligned} f_q &= (1.07 \pm 0.02) f_\pi, \\ f_s &= (1.34 \pm 0.06) f_\pi, \\ \alpha &= 39.3^\circ \pm 1.0^\circ. \end{aligned} \quad (45)$$

Using (45), we determine the values of the three parameters

$$\begin{aligned} \omega_{\eta_q} &= 1.215 \text{ GeV}, \\ m_s &= 0.262 \text{ GeV}, \\ \omega_{\eta_s} &= 1.229 \text{ GeV}, \end{aligned} \quad (46)$$

and calculate the transition form factors  $F_{\eta\gamma}(Q^2)$  and  $F_{\eta'\gamma}(Q^2)$ . The value of the parameter  $m_s$  is a little smaller than the order of 0.4 GeV. The results are plotted in Figs. 5 and 6 and are both in agreement with the data. The Gaussian-type wavefunction has been used in [18]; there the decay widths  $\Gamma(\eta^{(\prime)} \rightarrow \gamma\gamma)$  were obtained using the axial anomaly plus PCAC relations, and an  $q^2$  dependence [32] results with mixing angle  $\theta_{SU(3)} = -19^\circ$ .

Comparing with the predictions of pQCD [42–45], they fit the data well in the  $-16 \text{ GeV}^2 \leq q^2 \leq -1 \text{ GeV}^2$  region for  $F_{\eta\gamma}(Q^2)$  and  $F_{\eta'\gamma}(Q^2)$ . A nontrivial quark–antiquark structure of the photon is suggested and combined with the pQCD method to evaluate the transition form factors of  $\pi$ ,  $\eta$ , and  $\eta'$  [46]; the results are in agreement with the data in the  $-16 \text{ GeV}^2 \leq q^2 \leq 0$  region.

## 4 Conclusion

The charge and transition form factors of the light mesons are studied in the present paper. In the relativistic light-front quark model, these form factors have been evaluated

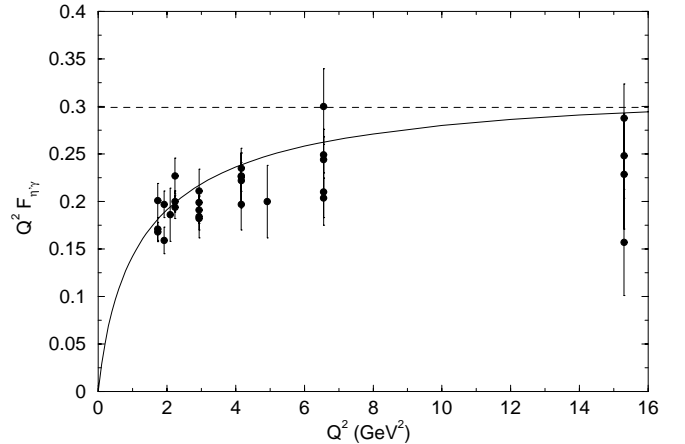


**Fig. 6.** The one off-shell photon transition form factor of  $\eta'$ . The dotted line is the limiting behavior (0.300 GeV) which is predicted by pQCD. Data are taken from [28]

in the frame where  $q^+ = 0$  and  $q^2 \leq 0$  and there is no need to calculate the contribution from the so-called Z graph [20].

We have used the experimental values of the decay constant  $f_\pi$ , the electromagnetic radius  $\langle r^2 \rangle_\pi$ , and the decay width  $\Gamma(\pi \rightarrow \gamma\gamma)$  as the constraints to fix the parameters appearing in the pion wavefunction. When the parameters are fixed, we evaluate the charge as well as one and two virtual photon transition form factors. Comparing the results of the calculation with the experimental data, we find that the fitted parameters are applicable in the  $-8 \text{ GeV}^2 \leq q^2 \leq 0$  region for both charge and transition form factors. Thus, the assumption is satisfied: the wavefunction is process independent. For the  $\eta$ – $\eta'$  system, a similar method for fixing the parameters is used. We also find that the results  $F_{\eta\gamma}(Q^2)$  and  $F_{\eta'\gamma}(Q^2)$  are in agreement with the experimental data. From these results, it is seen that LFQM is valid up to the scale of order  $Q^2 \sim 16 \text{ GeV}^2$ ; however, the constituent quark models are only applicable in the low-energy region. When  $Q^2 \rightarrow \infty$ , the method of pQCD will be suitable and the light quark masses are almost equal to zero. Thus, evolution of parameter values and distribution functions between the low  $Q^2$  and large  $Q^2$  regions [47] can be expected and seems to be interesting.

In principle, the wavefunction must be solved by the bound state equations. Before getting it from first principle, the phenomenological wavefunctions are needed. However, finding the wavefunction which can fit all the experimental data is not easy. This work reveals that the power-law wavefunction and the new treatment of the  $\eta$ – $\eta'$  mixing system are suitable for use in the two photons decay and the transition form factors of the light mesons. The major difference between the power-law- and Gaussian-type wavefunctions are the behaviors of the transverse momentum suppression. Thus, further, we can use these wavefunctions for the other processes to realize the adaptability of the light-front dynamics.

*Acknowledgements.* We are grateful to T. Feldmann and H.Y. Cheng for helpful discussions on the  $\eta$ - $\eta'$  mixing system. This work was supported in part by the National Science Council of ROC under Contract Nos. NSC89-2112-M-009-035 and NSC89-2112-M-007-054.

## References

1. D. Daniel et al., Phys. Rev. D **43**, 3715 (1991)
2. J. Gao, B.A. Li, Phys. Rev. D **61**, 113006 (2000)
3. Ll. Ametller et al., Phys. Rev. D **45**, 986 (1992)
4. G.P. Lepage, S.J. Brodsky, Phys. Rev. D **22**, 2157 (1980)
5. H.N. Li, G. Sterman, Nucl. Phys. B **381**, 129 (1992)
6. P. Kessler, S. Ong, Phys. Rev. D **48**, R2974 (1993); S. Ong, Phys. Rev. D **52**, 3111 (1995)
7. F.G. Cao, T. Huang, B.Q. Ma, Phys. Rev. D **53**, 6582 (1996)
8. M.A. Shifman, A.I. Vainshtein, V.I. Zakharov, Nucl. Phys. B **147**, **385**, 448 (1979)
9. V.M. Braun, I. Halperin, Phys. Lett. B **328**, 457 (1994)
10. A. Khodjamirian, Eur. Phys. J. C **6**, 477 (1999)
11. I.V. Anikin, A.E. Dorokhov, L. Tomio, Phys. Lett. B **475**, 361 (2000)
12. P.L. Chung, F. Coester, W.N. Polyzou, Phys. Lett. B **205**, 545 (1988)
13. F. Cardarelli et al., Phys. Rev. D **53**, 6682 (1996)
14. W. Jaus, Phys. Rev. D **41**, 3394 (1990); *ibid.* D **44**, 2851 (1991); Z. Phys. C **54**, 611 (1992)
15. P.J. O'Donnell et al., Phys. Lett. B **325**, 219 (1994); Phys. Lett. B **336**, 113 (1994); Phys. Rev. D **52**, 3966 (1995)
16. N.B. Demchuk et al., Phys. Atom. Nucl **59**, 2152 (1996)
17. H.M. Choi, C.R. Ji, Phys. Rev. D **56**, 6010 (1997)
18. H.M. Choi, C.R. Ji, Phys. Rev. D **59**, 074015 (1999)
19. C.Y. Cheung, C.W. Hwang, W.M. Zhang, Z. Phys. C **75**, 657 (1997)
20. H.Y. Cheng, C.Y. Cheung, C.W. Hwang, Phys. Rev. D **55**, 1559 (1997)
21. M. Sawicki, Phys. Rev. D **44**, 433 (1991)
22. M. Diehl, Th. Feldmann, R. Jakob, P. Kroll, hep-ph/0009255
23. W.M. Zhang, Chin. J. Phys. **31**, 717 (1994); Phys. Rev. D **56**, 1528 (1997)
24. S.R. Amendolia et al. (NA7 Coll.), Nucl. Phys. B **277**, 168 (1986)
25. C.J. Bebek et al., Phys. Rev. D **17**, 1693 (1978)
26. J. Volmer et al., nucl-ex/0010009
27. P. Brauel et al., Z. Phys. C **3**, 101 (1979)
28. CLEO Collaboration, Phys. Rev. D **57**, 33 (1998)
29. C.Y. Cheung, W.M. Zhang, G.L. Lin, Phys. Rev. D **52**, 2915 (1995)
30. B. Chibisov, A.R. Zhitnitsky, Phys. Rev. D **52**, 5273 (1995)
31. S.J. Brodsky, hep-ph/9807212
32. H.M. Choi, C.R. Ji, Nucl. Phys. A **618**, 291 (1997)
33. G. Köpp, T.F. Walsh, P. Zerwas, Nucl. Phys. B **70**, 461 (1974)
34. E.B. Dally et al., Phys. Rev. Lett. **48**, 375 (1982)
35. C. Caso et al., Eur. Phys. J. C **3**, 1 (1998)
36. S.J. Brodsky, G.P. Lepage, Phys. Rev. D **24**, 1808 (1981)
37. P. Maris, C.D. Roberts, Phys. Rev. C **58**, 3659 (1998)
38. B. Melic, B. Nizic, K. Passek, Phys. Rev. D **60**, 074004 (1999)
39. P. Kroll, M. Raulfs, Phys. Lett. B **387**, 848 (1996)
40. I.V. Musatov, A.V. Radyushkin, Phys. Rev. D **56**, 2713 (1997)
41. H. Leutwyler, Nucl. Phys. (Proc. Suppl.) **64**, 223 (1998); R. Kaiser, diploma work, Bern University, 1997
42. T. Feldmann, P. Kroll, Eur. Phys. J. C **5**, 327 (1998)
43. T. Feldmann, P. Kroll, B. Stech, Phys. Rev. D **58**, 114006 (1998)
44. T. Feldmann, P. Kroll, Phys. Rev. D **58**, 057501 (1998)
45. T. Feldmann, Nucl. Phys. (Proc. Suppl.) **82**, 331 (2000)
46. V.V. Anisovich, D.I. Melikhov, V.A. Nikonov, Phys. Rev. D **55**, 2918 (1997)
47. C. Vogt, hep-ph/0007277